

# SCIENTIFIC REPORTS

OPEN

## Coexistence of superconductivity and ferromagnetism in $\text{Sr}_{0.5}\text{Ce}_{0.5}\text{FBiS}_{2-x}\text{Se}_x$ ( $x = 0.5$ and $1.0$ ), a non-U material with $T_c < T_{\text{FM}}$

Received: 11 May 2016  
Accepted: 31 October 2016  
Published: 28 November 2016

Gohil S. Thakur<sup>1</sup>, G. Fuchs<sup>2</sup>, K. Nenkov<sup>2</sup>, Zeba Haque<sup>1</sup>, L. C. Gupta<sup>1,†</sup> & A. K. Ganguli<sup>1,3</sup>

We have carried out detailed magnetic and transport studies of the new  $\text{Sr}_{0.5}\text{Ce}_{0.5}\text{FBiS}_{2-x}\text{Se}_x$  ( $0.0 \leq x \leq 1.0$ ) superconductors derived by doping Se in  $\text{Sr}_{0.5}\text{Ce}_{0.5}\text{FBiS}_2$ . Se-doping produces several effects: it suppresses semiconducting-like behavior observed in the undoped  $\text{Sr}_{0.5}\text{Ce}_{0.5}\text{FBiS}_2$ , the ferromagnetic ordering temperature,  $T_{\text{FM}}$ , decreases considerably from 7.5 K (in  $\text{Sr}_{0.5}\text{Ce}_{0.5}\text{FBiS}_2$ ) to 3.5 K and the superconducting transition temperature,  $T_c$ , gets enhanced slightly to 2.9–3.3 K. Thus in these Se-doped materials,  $T_{\text{FM}}$  is marginally higher than  $T_c$ . Magnetization studies provide evidence of bulk superconductivity in  $\text{Sr}_{0.5}\text{Ce}_{0.5}\text{FBiS}_{2-x}\text{Se}_x$  at  $x \geq 0.5$  in contrast to the undoped  $\text{Sr}_{0.5}\text{Ce}_{0.5}\text{FBiS}_2$  ( $x = 0$ ) where magnetization measurements indicate a small superconducting volume fraction. Quite remarkably, as compared with the effective paramagnetic Ce-moment ( $\sim 2.2 \mu_B$ ), the ferromagnetically ordered Ce-moment in the superconducting state is rather small ( $\sim 0.1 \mu_B$ ) suggesting itinerant ferromagnetism. To the best of our knowledge,  $\text{Sr}_{0.5}\text{Ce}_{0.5}\text{FBiS}_{2-x}\text{Se}_x$  ( $x = 0.5$  and  $1.0$ ) are distinctive Ce-based bulk superconducting itinerant ferromagnetic materials with  $T_c < T_{\text{FM}}$ . Furthermore, a novel feature of these materials is that they exhibit a dual and quite unusual hysteresis loop corresponding to both the ferromagnetism and the coexisting bulk superconductivity.

Traditionally, superconductivity and long-range ferromagnetism had been considered mutually exclusive (BCS pair-breaking and Meissner effect). For example, in several ternary materials  $\text{RMO}_6\text{X}_8$  ( $X = \text{S}, \text{Se}$ )<sup>1</sup> and  $\text{RRh}_4\text{B}_4$ <sup>2,3</sup>, studied in the early eighties, superconductivity was observed coexisting with long range antiferromagnetic order. But uniform ferromagnetism suppressed superconductivity at low temperatures<sup>4–6</sup>. The situation has changed strikingly over the last several years with the discovery of a number of materials that do exhibit coexistence of superconductivity and long-range ferromagnetism. In materials such as  $\text{ErNi}_2\text{B}_2\text{C}$ <sup>7,8</sup> and  $\text{RuSr}_2\text{GdCu}_2\text{O}_8$ <sup>9</sup>, localized  $4f$ -moments (Er, Gd) are responsible for long-range ferromagnetism whereas  $3d$ -conduction electrons carry superconductivity. In certain U-containing materials, such as  $\text{UGe}_2$ <sup>10</sup>,  $\text{URhGe}$ <sup>11</sup>,  $\text{UIr}$ <sup>12</sup>,  $\text{UCoGe}$ <sup>13</sup>, the situation is drastically different. Here U- $5f$  itinerant electrons are responsible for both superconductivity and ferromagnetism. These materials, with  $T_{\text{FM}} > T_{\text{SC}}$ , present an unusual and surprising scenario of coexistence, namely, superconductivity setting in an already ferromagnetically ordered host. In such cases, spin-triplet pairing ( $p$ -wave superconductivity) has been suggested (U-compounds such as  $\text{UCoGe}$ ,  $\text{URhGe}$  and  $\text{UGe}_2$  have been proposed/considered  $p$ -wave ferromagnetic superconductors)<sup>14</sup> to be compatible with itinerant ferromagnetism. For  $p$ -wave pairing, one needs to go beyond electron-phonon interaction (pairing mechanism in conventional superconductivity) with Cooper-pairing mediated via spin fluctuations. The material  $\text{UCoGe}$  is of particular interest from the viewpoint of the present work. In this material the paramagnetic effective moment of U is  $\sim 1.7 \mu_B$  whereas the ferromagnetic ordered moment of U is drastically reduced,  $0.03 \mu_B$ <sup>13</sup>. The materials under investigation (the title compounds) in this work, exhibit coexisting superconductivity and itinerant ferromagnetic properties, as we shall see below, similar to those of  $\text{UCoGe}$ .

The parent material  $\text{Sr}_{0.5}\text{Ce}_{0.5}\text{FBiS}_2$  of the title compounds  $\text{Sr}_{0.5}\text{Ce}_{0.5}\text{FBiS}_{2-x}\text{Se}_x$  belongs to a small class  $\text{AFBiS}_2$  ( $A = \text{Sr}$  and  $\text{Eu}$ )<sup>15,16</sup> of a larger family of  $\text{BiS}_2$  layered tetragonal materials  $\text{LnOBiS}_2$ <sup>17,18</sup> ( $P4/nmm$ ) recently shown

<sup>1</sup>Department of Chemistry, Indian Institute of Technology, New Delhi, 110016, India. <sup>2</sup>Leibniz-Institut für Festkörper- und Werkstoffforschung Dresden, 01069, Germany. <sup>3</sup>Institute of Nano Science and Technology, Mohali, Punjab, 160064, India. <sup>†</sup>Present address: Solid State and Nano Research laboratory, Dept. of Chemistry, IIT Delhi. Correspondence and requests for materials should be addressed to A.K.G. (email: ashok@chemistry.iitd.ac.in)

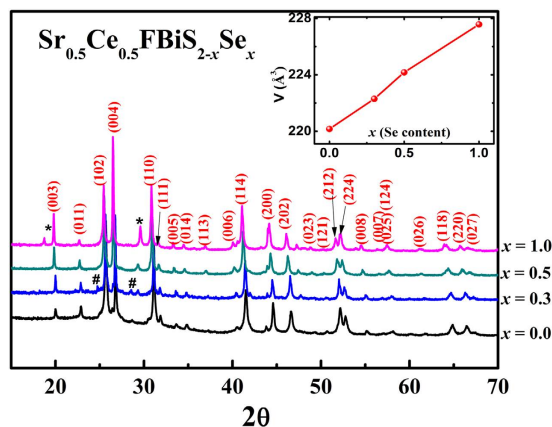


**Figure 1.** Powder X-ray diffraction of  $\text{Sr}_{0.5}\text{Ce}_{0.5}\text{FBiS}_{2-x}\text{Se}_x$  ( $x = 0.0, 0.3, 0.5$  and  $1.0$ ). Symbols (\*) and (#) indicate impurity phases  $\text{Bi}_2\text{Se}_3$  and  $\text{Bi}_2\text{S}_3$  respectively. Inset shows the variation of cell volume with Se content.

to exhibit superconductivity<sup>19–25</sup>.  $\text{SrFBiS}_2$  is derived by replacing Ln–O layers by Sr–F layers. Its structure essentially consists of alternate stacking of conducting  $\text{BiS}_2$  layers and blocking (insulating) layer  $\text{LnO/SrF}$ <sup>15,17,19</sup>. Electron carriers are doped into the superconducting  $\text{BiS}_2$  layers employing the commonly used doping strategy, namely, replacing O partially by F, for instance  $\text{LaO}_{0.5}\text{F}_{0.5}\text{BiS}_2$  exhibits superconductivity at  $T_c \sim 2.8$  K<sup>19</sup>. In  $\text{AFBiS}_2$ , electron doping and eventual superconductivity is achieved/enhanced by Ln (La and Ce) doping at A sites<sup>26–29</sup>. Structurally, these materials are quite similar to high- $T_c$  cuprates and iron pnictides and superconductivity is quite robust as evident from numerous studies on various site substitutions<sup>24,30–32</sup>.  $T_c$  is enhanced in  $\text{LnO}_{1-x}\text{F}_x\text{BiS}_2$  by chemical pressure via partial or complete substitution of La by a smaller rare-earth (Ln = Ce, Pr, Nd, Sm and Yb)<sup>23,33–36</sup>.  $\text{YbO}_{0.5}\text{F}_{0.5}\text{BiS}_2$  has the highest  $T_c = 5.4$  K among  $\text{LnO}_{1-x}\text{F}_x\text{BiS}_2$  and, interestingly, it undergoes an anti-ferromagnetic transition ( $T_N \sim 2.7$  K) also<sup>23</sup>. Se substitution has been realized in  $\text{LaO}_{0.5}\text{F}_{0.5}\text{BiS}_{2-x}\text{Se}_x$ <sup>37</sup> where an enhancement of  $T_c$  is observed with maximum  $T_c$  of 3.8 K for  $\text{LaO}_{0.5}\text{F}_{0.5}\text{BiS}_2$  composition ( $x = 1.0$ ).  $T_c$  decreases on further Se substitution. For other rare earths (Ce and Nd), however, the effect of Se on  $T_c$  is different. In  $\text{Ce(O/F)BiS}_2$  enhancement in  $T_c$  is only marginal (2.4 to 2.6 K)<sup>38</sup>. Se substitution induces bulk superconductivity in La and Ce materials. In  $\text{Nd(O/F)BiS}_2$  and  $\text{Bi}_4\text{O}_4\text{S}_3$ , Se doping has been shown to depress  $T_c$ <sup>32,39</sup>. Se substitution in  $\text{AFBiS}_2$  has not been tried so far. Under applied pressure,  $T_c$  is enhanced in  $\text{LnO}_{1-x}\text{F}_x\text{BiS}_2$  and  $\text{A}_{1-x}\text{Ln}_x\text{FBiS}_2$  (Ln = La, Ce, Pr and Nd; A = Sr and Eu) upto a maximum of 10 K<sup>40–46</sup>. The  $\text{Bi-S}_2$  materials are BCS-like and probably have *s*-wave pairing symmetry<sup>47–51</sup>. But there is yet no consensus on the origin of superconductivity in these materials<sup>31</sup>.

Very recently, ferromagnetism and superconductivity have been reported to coexist in  $\text{CeO}_{1-x}\text{F}_x\text{BiS}_2$  and  $\text{Sr}_{1-x}\text{Ce}_x\text{FBiS}_2$  with  $T_c \sim 2.5$ –4 K and  $T_{\text{FM}} \sim 4$ –8 K<sup>20,27,52–54</sup>. As these materials have layered structure, magnetism originates in the Ce–O (or Sr/Ce–F) layers and conduction occurs in  $\text{BiS}_2$  layers. In  $\text{Sr}_{0.5}\text{Ce}_{0.5}\text{FBiS}_2$ , the parent materials for our Se-added materials  $\text{Sr}_{0.5}\text{Ce}_{0.5}\text{FBiS}_{2-x}\text{Se}_x$ , Ce-substitution provides conduction electrons as well as gives rise to long range magnetic order<sup>27</sup>. Ferromagnetic order takes place at a higher temperature (7.5 K) and superconductivity sets in at a lower temperature (2.8 K) in an already ferromagnetically ordered lattice. We report here the effect of substitution of larger isovalent Se ion at the S site on the magnetic and superconducting properties of  $\text{Sr}_{0.5}\text{Ce}_{0.5}\text{FBiS}_2$ . Se-doping leads to a modest enhancement of  $T_c$  (upto 3.3 K) and a significant depression of  $T_{\text{FM}}$  (down to 3.5 K). Thus Se-doping moves  $T_c$  and  $T_{\text{FM}}$  in opposite directions, bringing them in closer proximity in temperature. We believe the ferromagnetism in our materials is itinerant just as it is in  $\text{UCoGe}$ <sup>13</sup>, namely, high Ce-paramagnetic moment ( $\sim 2.2 \mu_B$ ) and small saturation Ce-magnetic moment (0.1  $\mu_B$ ). To the best of our knowledge, the materials  $\text{Sr}_{0.5}\text{Ce}_{0.5}\text{FBiS}_{2-x}\text{Se}_x$ ,  $x = 0.5, 1.0$  are unique Ce-containing materials exhibiting coexisting bulk superconductivity and itinerant ferromagnetism. Thus our observation of the coexistence of superconductivity and itinerant ferromagnetism in  $\text{Sr}_{0.5}\text{Ce}_{0.5}\text{FBiS}_{2-x}\text{Se}_x$  is a timely discovery, in that it puts U- and Ce on equal footing in this respect also.

## Results and Discussion

**PXRD characterization.** PXRD patterns of all the  $\text{Sr}_{0.5}\text{Ce}_{0.5}\text{FBiS}_{2-x}\text{Se}_x$  ( $x = 0.0, 0.3, 0.5$  and  $1.0$ ) compositions are shown in Fig. 1. All the peaks could be easily indexed on the basis of a  $\text{SrFBiS}_2$  type tetragonal unit cell (SG:  $P4/nmm$ ). Minor peaks corresponding to the impurity of  $\text{Bi}_2\text{S}_3$  (#) and  $\text{Bi}_2\text{Se}_3$  (\*) were also observed for composition with  $x > 0$ . The estimated impurity phase of  $\text{Bi}_2\text{S}_3$  was  $\sim 4\%$  observed in  $x = 0.3$  composition whereas the amount of  $\text{Bi}_2\text{Se}_3$  was  $\sim 6\%$  and  $\sim 14\%$  in  $x = 0.5$  and  $x = 1.0$  composition respectively. It is evident from X-ray studies that the impurities increase with the increase of Se content. The samples with  $x > 1.0$  were obtained as multiphase products. This indicates a Se solubility limit of  $x \sim 1.0$ . Lattice parameters *a* and *c* show an expected increase upon Se doping ( $a = 4.0886(2)$  Å,  $c = 13.4143(8)$  Å for  $x = 0.5$  and  $a = 4.1057(1)$  Å,  $c = 13.4756(8)$  Å for  $x = 1.0$ ) resulting in the monotonous unit cell expansion (inset in Fig. 1). Compositional analysis on  $x = 0.5$  and  $1.0$  samples gives a stoichiometry close to the nominal value for both the compositions (Figure S1 in supplementary material (SM)). For  $x = 1.0$  sample, the Se:S ratio was slightly less than 1, possibly due to the formation of small amount of the impurity phase  $\text{Bi}_2\text{Se}_3$ , which is non-magnetic and insulating under ambient pressure<sup>55</sup>. It does not interfere with superconducting and magnetic properties of the materials under investigation.

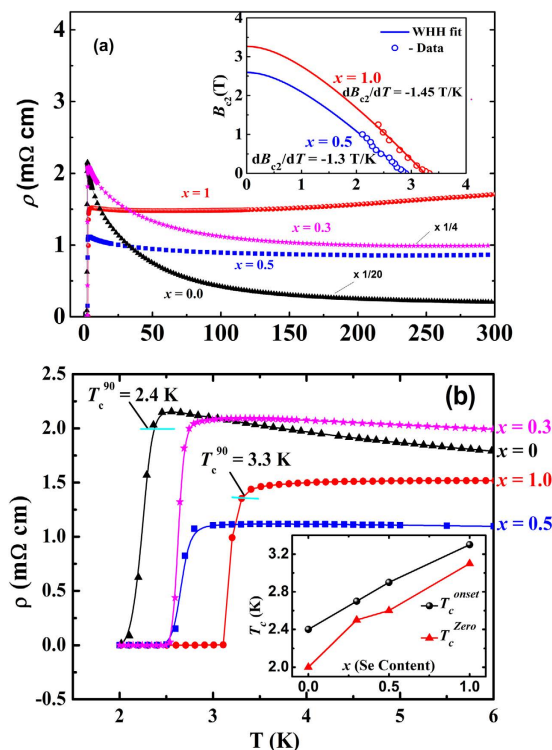


**Figure 2.** Variable temperature resistivity curves for  $\text{Sr}_{0.5}\text{Ce}_{0.5}\text{FBiS}_2-x\text{Se}_x$ ;  $x = 0, 0.3, 0.5$  and  $1.0$ . The data for  $x = 0$  and  $0.3$  have been divided by  $20$  and  $4$  respectively (a) in temperature range  $2$ – $300$  K and (b) in low temperature range. Inset of (a) shows the upper critical field ( $B_{c2}$ ) versus temperature ( $T$ ) curve for the  $x = 0.5$  and  $1.0$  compositions (open circles) along with the WHH fit (solid lines). Inset of (b) shows the variation of  $T_c^{\text{onset}}$  and  $T_c^{\text{zero}}$  as a function of Se-doping.

**Resistivity.** Resistivity of the materials as a function of temperature is shown in Fig. 2. In the normal state, resistivity of  $\text{Sr}_{0.5}\text{Ce}_{0.5}\text{FBiS}_{2-x}\text{Se}_x$  with  $x = 0$  and  $0.3$  exhibit semiconducting-like temperature dependence, namely, it increases with the decrease of temperature just before the onset of superconducting transition at  $2.4$  K and  $2.7$  K respectively as shown in Fig. 2(a). Note that the resistivity values for  $x = 0$  and  $0.3$  were divided by a factor of  $20$  and  $4$  respectively for the purpose of clarity. In the higher Se-doped materials,  $x = 0.5$  and  $x = 1.0$ , this semiconducting behavior is progressively subdued and metallic conductivity is observed in the normal state. Superconductivity sets in at  $T_c = 2.9$  and  $3.3$  K in materials with  $x = 0.5$  and  $1.0$  respectively. Our estimate of  $T_c^{\text{onset}}$  is based on a  $90\%$  criterion as shown in Fig. 2(b). Se-doping clearly enhances  $T_c$  by  $\sim 1$  K (inset of Fig. 2(b)). In the material with  $x = 1.0$ , a sharp superconducting transition is observed with a transition width  $\Delta T = 0.2$  K. Similar small enhancement in  $T_c$  with Se substitution was previously observed in  $\text{LnO}_{1-x}\text{F}_x\text{BiS}_2$  ( $\text{Ln} = \text{La}$  and  $\text{Ce}$ )<sup>38,56,57</sup>. This enhancement in  $T_c$  is attributed to the in-plane chemical pressure induced by the Se substitution at S sites as elucidated by Mizuguchi *et al.*<sup>58</sup>. The plot of upper critical field,  $B_{c2}(T)$  as a function of temperature is given in the inset of Fig. 2(a). We estimated  $B_{c2}$  below  $2$  K using a standard single-band Werthamer–Helfand–Hohenberg (WHH) formula with the Maki parameter<sup>59</sup>  $\alpha = 0$ . Upper critical field,  $B_{c2}(0)$  at  $T = 0$  is estimated to be  $2.6$  T for  $x = 0.5$  and  $3.3$  T for  $x = 1.0$ . These  $B_{c2}$  values are at least twice higher than those reported for the Se-free samples  $\text{Sr}_{0.5}\text{Ln}_{0.5}\text{FBiS}_2$ <sup>26,27</sup>. Enhancement of  $T_c$  and  $B_{c2}$  in the Se-doped samples clearly indicates that Se atoms have entered the lattice. Enhancement of  $B_{c2}$  implies reduction of the coherence length or stronger impurity scattering due to Se doping in  $\text{Sr}_{0.5}\text{Ce}_{0.5}\text{FBiS}_2$ .

**Magnetic susceptibility in low field of 10 Oe.** Figure 3(a) shows dc susceptibility of  $\text{Sr}_{0.5}\text{Ce}_{0.5}\text{FBiS}_{2-x}\text{Se}_x$  ( $x = 0.5$  and  $1.0$ ), in both the field-cooled (FC) and the zero field-cooled (ZFC) conditions in an applied field of  $10$  Oe. Clear diamagnetic signal, of magnitude close to the theoretical value, for both the  $x = 0.5$  and  $1.0$  compositions is observed in ZFC condition (Fig. 3a) establishing the superconducting state. Poor Meissner response in both cases is possibly due to flux pinning. A superconducting volume fraction of  $>95\%$  is estimated for both  $x = 0.5$  and  $1.0$  compositions. In several studies<sup>60–65</sup> on a variety of materials, such large diamagnetic superconducting signals have been observed and have been considered suggesting bulk superconductivity therein. Inset of Fig. 3(a) shows dc susceptibility of the Se free sample  $\text{Sr}_{0.5}\text{Ce}_{0.5}\text{FBiS}_2$  ( $x = 0.0$ ) which shows a ferromagnetic behavior with Curie temperature  $\sim 7.5$  K, similar to that reported earlier by Li *et al.*<sup>27</sup>. A weak drop in the ZFC susceptibility below  $3$  K is due to the superconducting transition that was also observed in our resistivity measurements. Such a weak diamagnetic signal rules out bulk superconductivity in parent sample  $x = 0.0$  and is consistent with weak superconductivity. Figure 3(b) shows both the real and the imaginary parts of the ac susceptibility. A large superconducting screening indicates bulk superconductivity. Moreover a larger imaginary part of the

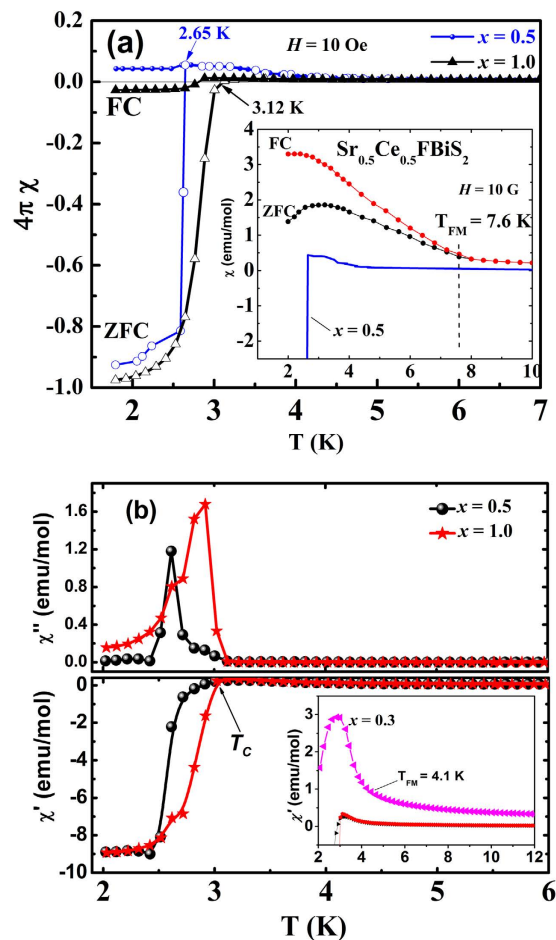


**Figure 3.** (a) Variable temperature  $dc$  susceptibility in ZFC and FC protocols for  $\text{Sr}_{0.5}\text{Ce}_{0.5}\text{FBiS}_{2-x}\text{Se}_x$  ( $x = 0.5, 1.0$ ) in an applied field of 10 Oe. Inset shows  $dc$  susceptibility for  $x = 0.0$  sample in comparison with  $x = 0.5$  sample in the same units (emu/mol) and (b) Real and imaginary parts of  $ac$  susceptibility for  $x = 0.5$  and 1.0 samples. Inset shows  $ac$  susceptibility for  $x = 0.3$  sample in comparison with  $x = 0.5$  and 1.0 samples.

signal indicates a considerable energy loss due to movement of vortices. Such a behavior cannot be explained if superconductivity is present only in thin surface layers. As deduced from these measurements, superconducting transition temperature increases from  $T_c^{\text{onset}} = 2.65$  K for  $x = 0.5$  to  $T_c^{\text{onset}} = 3.20$  K for  $x = 1$  which corroborates well with the resistivity data described above. It must be pointed out that in the earlier measurements on Se-free  $\text{Sr}_{0.5}\text{Ce}_{0.5}\text{FBiS}_2^{27,44}$  materials diamagnetic signal was not observed and the occurrence of superconductivity was inferred from the resistivity measurements only. Inset of Fig. 3b shows the low temperature  $ac$  susceptibility (real part) data for the compositions with  $x = 0.3$  in comparison with  $x = 0.5$  and 1.0 samples. It shows a ferromagnetic behavior similar to  $x = 0.0$  with a reduced Curie temperature  $T_{\text{FM}} = 4.1$  K. No diamagnetic signal was observed indicating that similar to the parent compound  $x = 0.3$  is also a weak superconductor. A clear diamagnetic signal is observed only for  $x = 0.5$  and 1.0 samples.

Further, in Fig. 3(a), a weak magnetic anomaly is discernible at 3.5 K for the sample  $x = 0.5$  which corresponds to a ferromagnetic transition as evidenced in our high field measurements, (see below), for both the samples  $x = 0.5$  and  $x = 1.0$ . This anomaly is not observed clearly for the sample  $x = 1.0$ .  $T_c$  and  $T_{\text{FM}}$  were ascertained from the derivative plots of susceptibility (see Figure S2 in SM). It is evident from the susceptibility studies that Se substitution depresses ferromagnetic ordering and enhances  $T_c$  in  $\text{Sr}_{0.5}\text{Ce}_{0.5}\text{FBiS}_{2-x}\text{Se}_x$ .

**High field DC magnetization measurements.** Magnetic susceptibility  $\chi(T)$ , measured in an applied field of 10 kOe, and its inverse in  $\text{Sr}_{0.5}\text{Ce}_{0.5}\text{FBiS}_{2-x}\text{Se}_x$  ( $x = 0.5$  and 1.0) is presented in the Figure S3 in SM. By fitting the data above 50 K to the Curie–Weiss law  $\chi(T) = \chi_0 + C/(T - \theta)$ , the paramagnetic effective magnetic moments obtained for the two samples are:  $\mu_{\text{eff}} = 2.22 \mu_B$  for  $x = 0.5$  and  $2.29 \mu_B$  for  $x = 1.0$  (see Figure S3 in SM). These values are close to the theoretical value  $2.54 \mu_B$  for free  $\text{Ce}^{3+}$  ions. Thus Ce-ions are in trivalent (or nearly trivalent state) state.

We display in Fig. 4 the results of our magnetization measurements, at a few selected temperatures 5 K, 3.5 K and 2 K, in  $\text{Sr}_{0.5}\text{Ce}_{0.5}\text{FBiS}_{1.5}\text{Se}_{0.5}$  and  $\text{Sr}_{0.5}\text{Ce}_{0.5}\text{FBiS}\text{Se}$ . At 5 K, magnetization  $M$  varies linearly with applied magnetic field, suggesting a paramagnetic state (no magnetic order). At 3.5 K,  $M$  is no longer linear in  $H$  in the low

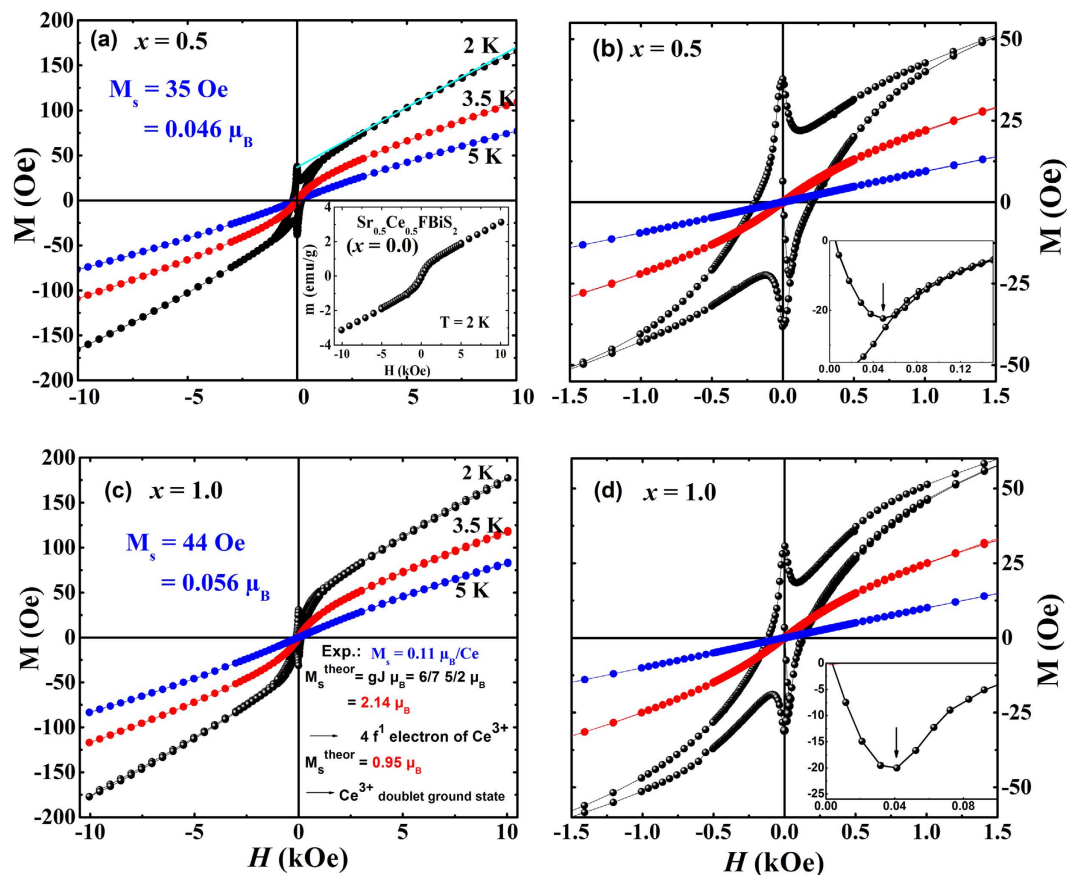


**Figure 4.** Hysteresis loops at different temperatures for  $\text{Sr}_{0.5}\text{Ce}_{0.5}\text{FBiS}_{1.5}\text{Se}_{0.5}$  and  $\text{Sr}_{0.5}\text{Ce}_{0.5}\text{FBiSSe}$  in  $H \leq 10$  kOe (a) and (c) and  $H \leq 1.5$  kOe (b) and (d). The superconducting loop is superimposed on the ferromagnetic loop at 2 K. Inset in Fig. 4(a) shows the ferromagnetic hysteresis loop for  $x = 0$  composition. Insets in Fig. 4(b) and (d) show initial diamagnetic signal with arrows indicating lower critical field,  $H_{cl}$ .

field region and shows a sign of a ferromagnetic behavior. Ferromagnetic state is clearly observed at a lower temperature 2 K and, remarkably, at this temperature in both the samples, we observe a ferromagnetic hysteresis loop and a superimposed superconducting hysteresis loop, demonstrating unambiguously the coexistence of ferromagnetism and bulk superconductivity. A dual loop, displaying the two ordered states, superconductivity and ferromagnetism, with such clarity, is a novel feature of this material. In  $\text{UCoGe}$ , ferromagnetic hysteresis is observed in the ferromagnetic state ( $T_c < T < T_{FM}$ ) but no superconducting hysteresis loop as such was observed<sup>66</sup>. Inset of Fig. 4a shows the isothermal magnetization (at 2 K) for  $x = 0$  where only a ferromagnetic hysteresis loop is observed. In the inset of Fig. 4(b) and (d) the diamagnetic response is clearly seen in the virgin low field region (from which  $H_{cl}$  is easily estimated to be  $\sim 44$  Oe and 40 Oe for  $x = 0.5$  and 1.0 respectively). It is important to point out that in the selenium-free compound  $\text{Sr}_{0.5}\text{Ce}_{0.5}\text{FBiS}_2$  ( $T_c \sim 2.6$  K &  $T_{FM} \sim 7.5$  K)<sup>27,44</sup> and in a similar material  $\text{Ce(O, F)BiS}_2$  ( $T_c \sim 2.5$ –4 K &  $T_{FM} \sim 6.5$ –7.5 K)<sup>20,52,53,67</sup> no superconducting hysteresis loop was observed. This is consistent with our own results on  $\text{Sr}_{0.5}\text{Ce}_{0.5}\text{FBiS}_2$  (inset of Fig. 4a). Thus Se-doping has created crucial changes in the superconducting and magnetic properties of the parent material  $\text{Sr}_{0.5}\text{Ce}_{0.5}\text{FBiS}_2$ . Observation of superconducting loop is a good indication of bulk superconductivity.

Dual hysteresis loop has been observed very recently in  $[(\text{Li}_{1-x}\text{Fe}_x)\text{OH}](\text{Fe}_{1-y}\text{Li}_y)\text{Se}$ <sup>68</sup>. However, there is a fundamental difference in this material and our samples, namely, in this case,  $T_c$  ( $\sim 43$  K)  $\gg T_{FM}$  (10 K) whereas in our case  $T_c < T_{FM}$  and hence, superconductivity sets in an already ferromagnetically ordered lattice. Further, in our case, superconductivity appears just at the border of ferromagnetic transition ( $T_{FM}$  is only marginally higher than  $T_c$ ) whereas in the above-mentioned material, superconductivity and ferromagnetism are far separated in temperature. In  $\text{CeFeAs}_{1-x}\text{P}_x\text{O}_{0.95}\text{F}_{0.05}$ , coexistence of superconductivity and ferromagnetism (with  $T_c > T_{FM}$ ) has been observed<sup>69</sup> in a limited doping range. In this case, however, Ce carries almost full moment and the system is not an itinerant ferromagnet.

The spontaneous magnetization  $M_s$  is estimated by linear extrapolation of the high-field data to  $H = 0$  (Fig. 4(a) and (c)). From the estimated  $M_s$ , we obtain at  $T = 2$  K, the spontaneous Ce-moment  $\mu_0 \sim 0.09 \mu_B$  for the sample  $x = 0.5$  and  $0.11 \mu_B$  for the sample  $x = 1.0$ . These values are quite small as compared with what is expected for free  $\text{Ce}^{3+}$  ion. We may note here that in  $\text{Ce(O, F)BiS}_2$  a reduced moment  $M_s = 0.52 \mu_B/\text{Ce}$  was reported<sup>53</sup> which, possibly, suggests that in this case Ce-ions may be in the crystal-field split doublet state (localized moment). In our case, we observe a drastically reduced, but non-zero, Ce-moment.

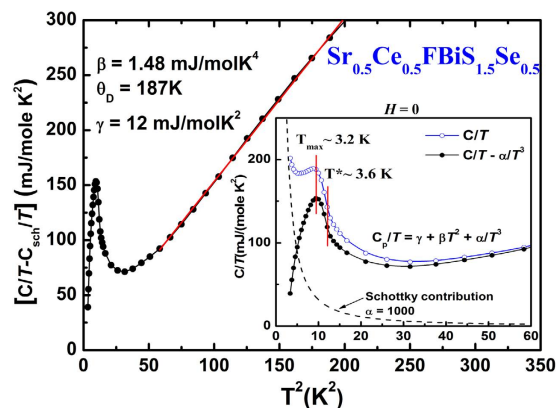


**Figure 5.** Temperature dependence of Schottky corrected specific heat  $C/T$  vs.  $T^2$  for  $x=0.5$  sample at  $H=0$ . Red line is the linear fit to the equation  $C/T = \gamma + \beta T^2$ . Inset shows  $C/T$  data before (blue circle) and after subtraction (black circle) of a Schottky contribution which is represented by the dashed line.

The transition of the high Ce-paramagnetic effective moment  $\mu_{\text{eff}} \sim 2.2 \mu_B$  to a small ordered moment  $\mu_0 \sim 0.1 \mu_B$  in the superconducting state is an important observation as the drastic loss of Ce-moment signals a delocalization of the  $4f$  electrons concurrent with the appearance of superconductivity. Thus,  $4f$ -electrons may also be involved in superconductivity in these materials. A *high* ratio  $\mu_{\text{eff}}/\mu_0$  ( $\sim 22$ ) implies an itinerant ferromagnetic state<sup>13,70</sup> in both materials  $\text{Sr}_{0.5}\text{Ce}_{0.5}\text{FBiS}_{2-x}\text{Se}_x$ ,  $x=0.5$  and  $x=1.0$ . Further, as Ce-atoms are responsible both for ferromagnetism and coexisting bulk superconductivity we think the two phenomena can coexist uniformly. These materials fill the glaring void, namely, so far no Ce-based material has been hitherto known exhibiting superconductivity within the itinerant ferromagnetic state.

**Specific heat.** Figure 5 shows the temperature dependence of specific heat of  $\text{Sr}_{0.5}\text{Ce}_{0.5}\text{FBiS}_{1.5}\text{Se}_{0.5}$  ( $x=0.5$ ) in the low temperature range 2–16 K. Inset shows  $C/T$  data before (blue circle) and after subtraction (black circle) of a Schottky contribution which was approximated by the dashed line. A broad peak, not  $\lambda$ -shaped as expected for a ferromagnet, centered at 3.2 K (inset of Fig. 5) is observed from which, following Li *et al.*<sup>27</sup>, ferromagnetic ordering temperature  $T_{\text{FM}} \sim 3.6$  K is obtained. As  $T_{\text{FM}}$  and  $T_c$  are quite close, separate anomalies of the two transitions, the magnetic and the superconducting, are not resolved. It should be pointed that in similar systems like  $\text{CeO}_{0.5}\text{F}_{0.5}\text{BiS}_2$  and  $\text{YbO}_{0.5}\text{F}_{0.5}\text{BiS}_2$  specific heat anomaly around  $T_c$  is not observed<sup>23</sup> and the anomaly observed in  $\text{Sr}_{0.5}\text{Ce}_{0.5}\text{FBiS}_2$  is extremely small<sup>53</sup>. Red line in the main panel of Fig. 5 obeys the equation:  $C/T = \gamma + \beta T^2$  yielding the Debye temperature  $\theta_D = 187$  K and the Sommerfeld coefficient  $\gamma = 12$  mJ/(K<sup>2</sup>mol Ce). This  $\gamma$  value of  $\text{Sr}_{0.5}\text{Ce}_{0.5}\text{FBiS}_{1.5}\text{Se}_{0.5}$  is much smaller than that of  $\text{Sr}_{0.5}\text{Ce}_{0.5}\text{FBiS}_2$  ( $\gamma = 117$  mJ/(K<sup>2</sup>mol Ce))<sup>27</sup>. However, it is larger by a factor of 5–10 as compared to  $\text{Sr}_{1-x}\text{La}_x\text{FBiS}_2$  ( $\gamma < 2$  mJ/mol-K<sup>2</sup>)<sup>26,71,72</sup> and  $\text{La}_{1-x}\text{M}_x\text{OBiS}_2$  ( $M = \text{Ti, Zr, Th}$ ) ( $\gamma \sim 0.58\text{--}2.21$  mJ/mol K<sup>2</sup>)<sup>24</sup>. Ce  $4f$ -electrons are responsible for the increased density of states at the Fermi level in  $\text{Sr}_{0.5}\text{Ce}_{0.5}\text{FBiS}_{1.5}\text{Se}_{0.5}$  as compared to that in other BiS<sub>2</sub> system without Ce. Therefore, the higher  $\gamma$  value in the normal state of  $\text{Sr}_{0.5}\text{Ce}_{0.5}\text{FBiS}_2$  is attributed to the electronic correlation effect of Ce- $4f$  electrons which are reduced in the Se-doped sample. From the specific heat measurements we get an entropy per Ce atom of only about 4% of the expected value for  $J = 5/2$ . The low magnetic entropy ( $S_m = 0.04R \ln 6$ ) is consistent with weak itinerant ferromagnetism in  $\text{Sr}_{0.5}\text{Ce}_{0.5}\text{FBiS}_{1.5}\text{Se}_{0.5}$ . This situation is similar to that in  $\text{UCoGe}$ <sup>13</sup>.

With the help of our experimental data, we construct a ferromagnetism/superconductivity phase diagram of the system  $\text{Sr}_{0.5}\text{Ce}_{0.5}\text{FBiS}_{2-x}\text{Se}_x$  ( $0 \leq x \leq 1$ ) which is shown in Fig. 6. Upon doping Se ferromagnetic ordering temperature ( $T_{\text{FM}}$ ) decrease along with a concomitant increase in the  $T_c$ . Ferromagnetism and weak superconductivity are observed for  $x < 0.5$ . In the two materials  $x=0.5$  and  $x=1.0$ , bulk superconductivity is observed coexisting with ferromagnetism. The dual hysteresis loops, shown in Fig. 4, are observed for these samples.  $T_{\text{FM}}$  and  $T_c$  lie in close proximity in the  $x=1.0$  composition.

After submission of this manuscript we came across a report on the coexistence of superconductivity and ferromagnetism in  $\text{CsEuFe}_4\text{As}_4$  compound<sup>73</sup>. A dual hysteresis loop has been observed in this compound also. The superconducting loop, however, is not so prominent. This remark has been added in the revised version of the manuscript.

## Concluding Remarks

We have observed superconductivity ( $T_c \sim 3.0$  K) and itinerant ferromagnetism ( $T_{\text{FM}} \sim 3.5$  K) coexisting in the new materials  $\text{Sr}_{0.5}\text{Ce}_{0.5}\text{FBiS}_{2-x}\text{Se}_x$  at  $x \geq 0.5$ . Thus in these materials, superconductivity occurs much closer to the border of ferromagnetism than in  $\text{UCoGe}$ . A novel feature of these materials, as compared with the other ferromagnetic superconductors reported so far, is a dual hysteresis loop corresponding to both the coexisting bulk superconductivity and ferromagnetism. Thus  $\text{Sr}_{0.5}\text{Ce}_{0.5}\text{FBiS}_{2-x}\text{Se}_x$  is an important and timely addition to the exciting Ce-based materials exhibiting coexisting superconductivity and magnetism. The materials  $\text{Sr}_{0.5}\text{Ce}_{0.5}\text{FBiS}_{2-x}\text{Se}_x$  are potential candidates for the unconventional  $p$ -wave superconductivity<sup>74</sup> and deserve to be further pursued in this regard. We are making efforts to grow single crystals of these materials. In single crystals (if we succeed to grow) or else in polycrystalline materials, we would carry out studies such as NMR,  $\mu\text{SR}$ , neutron diffraction

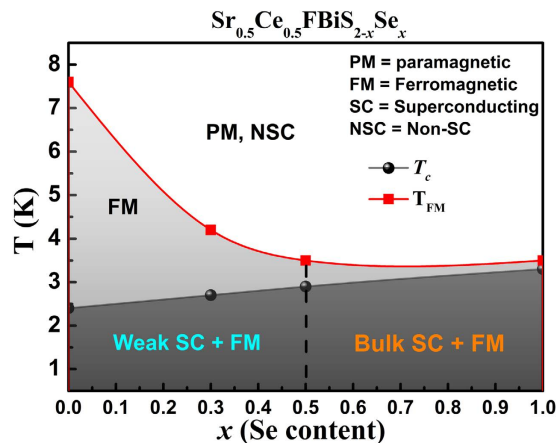


**Figure 6.** Ferromagnetism and superconductivity phase diagram of  $\text{Sr}_{0.5}\text{Ce}_{0.5}\text{FBiS}_{2-x}\text{Se}_x$  ( $0 \leq x \leq 1$ ).

and Andreev reflection to throw further light on the coexistence of superconductivity and ferromagnetism and nature of the superconducting state (*p*-wave or *s*-wave) in these materials.

## Methods

Polycrystalline compounds of the series  $\text{Sr}_{0.5}\text{Ce}_{0.5}\text{FBiS}_{2-x}\text{Se}_x$  ( $x = 0.0, 0.3, 0.5$  and  $1.0$ ) were prepared by the usual solid state synthesis procedure as reported elsewhere<sup>28,35</sup>.  $\text{SrF}_2$ , Bi and Se powder, pre-reacted  $\text{Ce}_2\text{S}_3$  and  $\text{Bi}_2\text{S}_3$  powder were thoroughly mixed, pelletized and sealed in quartz tube under vacuum. The tubes were then heated twice at  $800^\circ\text{C}$  for 24 hours with an intermediate grinding. The end products were black/dark grayish in color. Phase purity of all the compositions was checked by powder X-ray diffraction (PXRD) technique using Cu-K $\alpha$  radiation source. Temperature dependent resistivity, magnetization and specific heat measurements were performed using a 14 T PPMS (Quantum Design). The specific heat was measured using a relaxation technique.

## References

- Ishikawa, M. & Fischer, Ø. Magnetic ordering in the superconducting state of rare earth molybdenum sulphides (Re)1.2Mo6Se8 (Re = Tb, Dy and Er). *Solid State Commun.* **24**, 747 (1977).
- Rossel, C. Superconductivity in ternary compounds. *Nuovo Cim.* **2D**, 1834–1845 (1983).
- Hamaker, H. C., Woolf, L. D., MacKay, H. B., Fisk, Z. & Maple, M. B. Coexistence of Superconductivity and Antiferromagnetic Order in  $\text{SmRh}_4\text{B}_4$ . *Solid State Commun.* **32**, 289 (1980).
- Ishikawa, M. & Fischer, Ø. Destruction of superconductivity by magnetic ordering in  $\text{Ho}_{1.2}\text{Mo}_6\text{S}_8$ . *Solid State Commun.* **88**, 863–865 (1977).
- Fertig, W. A. *et al.* Destruction of superconductivity at the onset of long-range magnetic order in the compound  $\text{ErRh}_4\text{B}_4$ . *Phys. Rev. Lett.* **38**, 987–990 (1977).
- Ishikawa, M. Can magnetism and superconductivity coexist? *Contemp. Phys.* **23**, 443–468 (1982).
- Cho, B. K. *et al.* Magnetism and superconductivity in single-crystal  $\text{ErNi}_2\text{B}_2\text{C}$ . *Phys. Rev. B* **52**, 3684–3695 (1995).
- Canfield, P. C., Bud'ko, S. L. & Cho, B. K. Possible co-existence of superconductivity and weak ferromagnetism in  $\text{ErNi}_2\text{B}_2\text{C}$ . *Physica C* **262**, 249–254 (1996).
- Bernhard, C. *et al.* Coexistence of ferromagnetism and superconductivity in the hybrid ruthenate-cuprate compound  $\text{RuSr}_2\text{GdCu}_2\text{O}_8$  studied by muon spin rotation and dc magnetization. *Phys. Rev. B* **59**, 14099–14107 (1999).
- Saxena, S. *et al.* Superconductivity on the border of itinerant-electron ferromagnetism in  $\text{UGe}_2$ . *Nature* **406**, 587–592 (2000).
- Aoki, D. *et al.* Coexistence of superconductivity and ferromagnetism. *Nature* **413**, 613–615 (2001).
- Akazawa, T. *et al.* Pressure-induced superconductivity in ferromagnet UIr without inversion symmetry. *J. Phys. Condens. matter* **16**, L29 (2004).
- Huy, N. T. *et al.* Superconductivity on the border of weak itinerant ferromagnetism in  $\text{UCoGe}$ . *Phys. Rev. Lett.* **99**, 67006 (2007).
- Gasparini, A. *et al.* The Superconducting Ferromagnet  $\text{UCoGe}$ . *J. Low Temp. Phys.* **161**, 134–147 (2010).
- Lei, H., Wang, K., Abeykoon, M., Bozin, E. S. & Petrovic, C. New Layered Fluorosulfide  $\text{SrFBiS}_2$ . *Inorg. Chem.* **52**, 10685–10689 (2013).
- Zhai, H.-F. *et al.* Possible charge-density wave, superconductivity, and f-electron valence instability in  $\text{EuBiS}_2\text{F}$ . *Phys. Rev. B* **90**, 64518 (2014).
- Céolin, R. & Rodier, N. Structure cristalline de l'oxysulfure de cérium et de bismuth  $\text{CeBiOS}_2$ . *Acta Crystallogr. Sect. B Struct. Crystallogr. Cryst. Chem.* **32**, 1476–1479 (1976).
- Tanryverdiev, V. S., Aliev, O. M. & Aliev, I. I. Synthesis and physicochemical properties of  $\text{LnBiOS}_2$ . *Inorg. Mater.* **31**, 1497 (1995).
- Mizuguchi, Y. *et al.* Superconductivity in novel  $\text{BiS}_2$ -based layered superconductor  $\text{LaO}_{1-x}\text{F}_x\text{BiS}_2$ . *J. Phys. Soc. Japan* **81**, 114725 (2012).
- Xing, J., Li, S., Ding, X., Yang, H. & Wen, H. H. Superconductivity appears in the vicinity of semiconducting-like behavior in  $\text{CeO}_{1-x}\text{F}_x\text{BiS}_2$ . *Phys. Rev. B* **86**, 214518 (2012).
- Awana, V. P. S. *et al.* Appearance of superconductivity in layered  $\text{LaO}_{0.5}\text{F}_{0.5}\text{BiS}_2$ . *Solid State Commun.* **157**, 21–23 (2013).
- Demura, S. *et al.*  $\text{BiS}_2$ -based superconductivity in F-substituted  $\text{NdOBiS}_2$ . *J. Phys. Soc. Jpn* **82**, 33708 (2013).
- Yazici, D. *et al.* Superconductivity of F-substituted  $\text{LnOBiS}_2$  (Ln = La, Ce, Pr, Nd, Yb) compounds. *Philos. Mag.* **93**, 673–680 (2013).
- Yazici, D. *et al.* Superconductivity induced by electron doping in  $\text{La}_{1-x}\text{M}_x\text{OBiS}_2$  (M = Ti, Zr, Hf, Th). *Phys. Rev. B* **87**, 174512 (2013).
- Jha, R. & Awana, V. P. S. Superconducting properties of  $\text{BiS}_2$  based superconductor  $\text{NdO}_{1-x}\text{F}_x\text{BiS}_2$  ( $x = 0$  to  $0.9$ ). *Mater. Res. express* **1**, 16002 (2014).
- Lin, X. *et al.* Superconductivity induced by La doping in  $\text{Sr}_{1-x}\text{La}_x\text{FBiS}_2$ . *Phys. Rev. B* **87**, 020504(R) (2013).
- Li, L. *et al.* Coexistence of superconductivity and ferromagnetism in  $\text{Sr}_{0.5}\text{Ce}_{0.5}\text{FBiS}_2$ . *Phys. Rev. B* **91**, 14508 (2015).

28. Thakur, G. S. *et al.* Pressure enhanced superconductivity at 10 K in La doped EuBiS<sub>2</sub>F. *Supercond. Sci. Technol.* **28**, 115010 (2015).
29. Zhai, H.-F. *et al.* Coexistence of superconductivity and complex 4 f magnetism in Eu<sub>0.5</sub>Ce<sub>0.5</sub>BiS<sub>2</sub>F. *J. Phys. Condens. Matter* **27**, 385701 (2015).
30. Mizuguchi, Y. Review of superconductivity in BiS<sub>2</sub>-based layered materials. *J. Phys. Chem. Solids* **84**, 34–48 (2014).
31. Yazici, D., Jeon, I., White, B. D. & Maple, M. B. Superconductivity in layered BiS<sub>2</sub>-based compounds. *Phys. C Supercond. its Appl.* **514**, 218–236 (2015).
32. Hiroi, T., Kajitani, J., Omachi, A., Miura, O. & Mizuguchi, Y. Element Substitution Effect on Superconductivity in BiS<sub>2</sub>-Based NdO<sub>1-x</sub>F<sub>x</sub>BiS<sub>2</sub>. *J. Supercond. Nov. Magn.* **28**, 1149–1153 (2015).
33. Kajitani, J., Omachi, A., Hiroi, T., Miura, O. & Mizuguchi, Y. Chemical pressure effect on T<sub>c</sub> in BiS<sub>2</sub>-based Ce<sub>1-x</sub>Nd<sub>x</sub>O<sub>0.5</sub>F<sub>0.5</sub>BiS<sub>2</sub>. *Physica C* **504**, 33–35 (2014).
34. Kajitani, J., Hiroi, T., Omachi, A., Miura, O. & Mizuguchi, Y. Chemical pressure effect on superconductivity of BiS<sub>2</sub>-based Ce<sub>1-x</sub>Nd<sub>x</sub>O<sub>1-y</sub>F<sub>y</sub>BiS<sub>2</sub> and Nd<sub>1-z</sub>Sm<sub>z</sub>O<sub>1-y</sub>F<sub>y</sub>BiS<sub>2</sub>. *J. Phys. Soc. Japan* **84**, 44712 (2015).
35. Thakur, G. S. *et al.* Synthesis and Properties of SmO<sub>0.5</sub>F<sub>0.5</sub>BiS<sub>2</sub> and Enhancement in T<sub>c</sub> in La<sub>1-y</sub>SmyO<sub>0.5</sub>F<sub>0.5</sub>BiS<sub>2</sub>. *Inorg. Chem.* **54**, 1076–1081 (2015).
36. Fang, Y., Yazici, D., White, B. D. & Maple, M. B. Enhancement of superconductivity in La<sub>1-x</sub>Sm<sub>x</sub>O<sub>0.5</sub>F<sub>0.5</sub>BiS<sub>2</sub>. *Phys. Rev. B* **91**, 64510 (2015).
37. Hiroi, T., Kajitani, J., Omachi, A., Miura, O. & Mizuguchi, Y. Evolution of superconductivity in BiS<sub>2</sub>-based superconductor LaO<sub>0.5</sub>F<sub>0.5</sub>Bi(S<sub>1-x</sub>Sex)<sub>2</sub>. *J. Phys. Soc. Japan* **84**, 24723 (2015).
38. Mizuguchi, Y., Hiroi, T. & Miura, O. Superconductivity phase diagram of Se-substituted CeO<sub>0.5</sub>F<sub>0.5</sub>Bi(S<sub>1-x</sub>Sex)<sub>2</sub>. *J. Phys. Conf. Ser.* **683**, 12001 (2016).
39. Jha, R. & Awana, V. P. S. Effect of Se doping in recently discovered layered Bi<sub>4</sub>O<sub>4</sub>S<sub>3</sub> superconductor. *Physica C* **498**, 45–49 (2014).
40. Wolowicz, C. T., Yazici, D., White, B. D., Huang, K. & Maple, M. B. Pressure-induced enhancement of superconductivity and suppression of semiconducting behavior in LnO<sub>0.5</sub>F<sub>0.5</sub>BiS<sub>2</sub> (Ln = La, Ce) compounds. *Phys. Rev. B* **88**, 64503 (2013).
41. Jha, R., Kishan, H. & Awana, V. P. S. Effect of hydrostatic pressures on the superconductivity of new BiS<sub>2</sub> based REO<sub>0.5</sub>F<sub>0.5</sub>BiS<sub>2</sub> (RE = La, Pr and Nd) superconductors. *J. Phys. Chem. Solids* **84**, 17–23 (2014).
42. Tomita, T. *et al.* Pressure-Induced Enhancement of Superconductivity and Structural Transition in BiS<sub>2</sub>-Layered LaO<sub>1-x</sub>F<sub>x</sub>BiS<sub>2</sub>. *J. Phys. Soc. Japan* **83**, 63704 (2014).
43. Jha, R., Tiwari, B. & Awana, V. P. S. Impact of Hydrostatic Pressure on Superconductivity of Sr<sub>0.5</sub>La<sub>0.5</sub>F<sub>0.5</sub>BiS<sub>2</sub>. *J. Phys. Soc. Jpn* **83**, 63707 (2014).
44. Jha, R., Tiwari, B. & Awana, V. P. S. Appearance of bulk superconductivity under hydrostatic pressure in (RE = Ce, Nd, Pr, and Sm) compounds. *J. Appl. Phys.* **117**, 13901 (2015).
45. Thakur, G. S. *et al.* Pressure enhanced superconductivity at 10 K in La doped EuBiS<sub>2</sub>F. *Supercond. Sci. Technol.* **28**, 115010 (2015).
46. Guo, C. Y. *et al.* Evidence for two distinct superconducting phases in EuBiS<sub>2</sub>F under pressure. *Phys. Rev. B - Condens. Matter Mater. Phys.* **91**, 214512 (2015).
47. Yildirim, T. Ferroelectric soft phonons, charge density wave instability, and strong electron-phonon coupling in BiS<sub>2</sub> layered superconductors: A first-principles study. *Phys. Rev. B* **87**, 020506(R) (2013).
48. Liang, Y., Wu, X., Tsai, W. F. & Hu, J. Pairing symmetry in layered BiS<sub>2</sub> compounds driven by electron-electron correlation. *Front. Phys.* **9**, 194–199 (2014).
49. Lamura, G. *et al.* s-wave pairing in the optimally doped LaO<sub>0.5</sub>F<sub>0.5</sub>BiS<sub>2</sub> superconductor. *Phys. Rev. B* **88**, 180509 (2013).
50. Zeng, L. K. *et al.* Observation of anomalous temperature dependence of spectrum on small Fermi surfaces in a BiS<sub>2</sub>-based superconductor. *Phys. Rev. B* **90**, 54512 (2014).
51. Ye, Z. R. *et al.* Electronic structure of single-crystalline NdO<sub>0.5</sub>F<sub>0.5</sub>BiS<sub>2</sub> studied by angle-resolved photoemission spectroscopy. *Phys. Rev. B* **90**, 45116 (2014).
52. Jha, R. & Awana, V. P. S. Superconductivity in Layered CeO<sub>0.5</sub>F<sub>0.5</sub>BiS<sub>2</sub>. *J. Supercond. Nov. Magn.* **27**, 1–4 (2013).
53. Lee, J. *et al.* Coexistence of ferromagnetism and superconductivity in CeO<sub>0.3</sub>F<sub>0.7</sub>BiS<sub>2</sub>. *Phys. Rev. B* **90**, 224410 (2014).
54. Demura, S. *et al.* Coexistence of bulk superconductivity and ferromagnetism in CeO<sub>1-x</sub>F<sub>x</sub>BiS<sub>2</sub>. *J. Phys. Soc. Jpn* **84**, 24709 (2015).
55. Kong, P. P. *et al.* Superconductivity of the topological insulator Bi<sub>2</sub>Se<sub>3</sub> at high pressure. *J. Phys. Condens. Matter* **25**, 362204 (2013).
56. Krzton-Maziopa, A. *et al.* Superconductivity in a new layered bismuth oxyselelide: LaO<sub>0.5</sub>F<sub>0.5</sub>BiSe<sub>2</sub>. *J. Phys. Condens. matter* **26**, 215702 (2014).
57. Tanaka, M. *et al.* Site selectivity on chalcogen atoms in superconducting La(O, F)BiSSe. *Appl. Phys. Lett.* **106**, 112601 (2015).
58. Mizuguchi, Y. *et al.* In-plane chemical pressure essential for superconductivity in BiCh<sub>2</sub>-based (Ch: S, Se) layered structure. *Sci. Rep.* **5**, 14968 (2015).
59. Werthamer, N. R., Helfand, E. & Hohenberg, P. C. Temperature and Purity Dependence of the Superconducting Critical Field, H<sub>c2</sub>. III. Electron Spin and Spin-Orbit Effects. *Phys. Rev.* **147**, 295–302 (1966).
60. Sefat, A. S. *et al.* Superconductivity in LaFe<sub>1-x</sub>CoxAsO. *Phys. Rev. B* **78**, 104505 (2008).
61. Sales, B. C. *et al.* Bulk superconductivity at 14 K in single crystals of Fe<sub>1+y</sub>TexSe<sub>1-x</sub>. *Phys. Rev. B* **79**, 94521 (2009).
62. Zhu, X. *et al.* Transition of stoichiometric Sr<sub>2</sub>VO<sub>3</sub>FeAs to a superconducting state at 37.2 K. *Phys. Rev. B* **79**, 220512R (2009).
63. Morozov, I. *et al.* Single Crystal Growth and Characterization of Superconducting LiFeAs. *Cryst. Growth Des.* **10**, 4428–4432 (2010).
64. Ying, J. J. *et al.* Superconductivity and magnetic properties of single crystals of K<sub>0.75</sub>Fe<sub>1.66</sub>Se<sub>2</sub> and Cs<sub>0.81</sub>Fe<sub>1.61</sub>Se<sub>2</sub>. *Phys. Rev. B* **83**, 212502 (2011).
65. Mizuguchi, Y. *et al.* Superconductivity in Novel BiS<sub>2</sub>-Based Layered Superconductor LaO<sub>1-x</sub>F<sub>x</sub>BiS<sub>2</sub>. *J. Phys. Soc. Japan* **81**, 114725 (2012).
66. Aoki, D. & Flouquet, J. Ferromagnetism and Superconductivity in Uranium Compounds. *J. Phys. Soc. Japan* **81**, 11003 (2012).
67. Kajitani, J., Hiroi, T., Omachi, A., Miura, O. & Mizuguchi, Y. Increase in T<sub>c</sub> and change of crystal structure by high-pressure annealing in BiS<sub>2</sub>-based superconductor CeO<sub>0.3</sub>F<sub>0.7</sub>BiS<sub>2</sub>. *J. Supercond. Nov. Magn.* **28**, 1129 (2014).
68. Pachmayr, U. *et al.* Coexistence of 3d-Ferromagnetism and Superconductivity in [(Li<sub>1-x</sub>Fex)OH](Fe<sub>1-y</sub>Li<sub>y</sub>)Se. *Angew. chemie Int. Ed.* **54**, 293–297 (2015).
69. Luo, Y. *et al.* Interplay of superconductivity and Ce 4f magnetism in CeFeAs<sub>1-x</sub>PxO<sub>0.95</sub>F<sub>0.05</sub>. *Phys. Rev. B* **83**, 54501 (2011).
70. Rhodes, P. & Wohlfarth, E. P. The effective Curie-Weiss constant of ferromagnetic metals and alloys. *Proc. R. Soc. London* **273**, 247 (1963).
71. Li, Y. *et al.* Electronic phase diagram in a new BiS<sub>2</sub>-based Sr<sub>1-x</sub>LaxFBiS<sub>2</sub> system. *Supercond. Sci. Technol.* **27**, 35009 (2014).
72. Sakai, H. *et al.* Insulator-to-Superconductor Transition upon Electron Doping in a BiS<sub>2</sub>-Based Superconductor Sr<sub>1-x</sub>LaxFBiS<sub>2</sub>. *J. Phys. Soc. Japan* **83**, 14709 (2014).
73. Liu, Y. *et al.* A new ferromagnetic superconductor: CsEuFe<sub>4</sub>As<sub>4</sub>. *Sci. Bull.* **61**, 1213–1220 (2016).
74. Fay, D. & Appel, J. Coexistence of p-state superconductivity and itinerant ferromagnetism. *Phys. Rev. B* **22**, 3173 (1980).

## Acknowledgements

Author AKG thanks DST (Govt. of India) for partial financial assistance. GST and ZH thank CSIR and UGC (Govt. of India) respectively for fellowships. We thank Dr. V. Grinenko (IFW) for helping in carrying out the measurements and for helpful discussion. Authors at IIT Delhi thank PPMS EVERCOOL-II facility at IIT Delhi.



### Author Contributions

G.S.T. carried out the synthesis and preliminary characterization (XRD and EDX) with help of Z.H., G.F. and K.N. carried out the resistivity, magnetic and specific heat measurements. All authors reviewed the manuscript. A.K.G., L.C.G. and G.F. supervised the work.

### Additional Information

**Supplementary information** accompanies this paper at <http://www.nature.com/srep>

**Competing financial interests:** The authors declare no competing financial interests.

**How to cite this article:** Thakur, G. S. *et al.* Coexistence of superconductivity and ferromagnetism in  $\text{Sr}_{0.5}\text{Ce}_{0.5}\text{FBiS}_{2-x}\text{Se}_x$  ( $x = 0.5$  and  $1.0$ ), a non-U material with  $T_c < T_{\text{FM}}$ . *Sci. Rep.* **6**, 37527; doi: 10.1038/srep37527 (2016).

**Publisher's note:** Springer Nature remains neutral with regard to jurisdictional claims in published maps and institutional affiliations.



This work is licensed under a Creative Commons Attribution 4.0 International License. The images or other third party material in this article are included in the article's Creative Commons license, unless indicated otherwise in the credit line; if the material is not included under the Creative Commons license, users will need to obtain permission from the license holder to reproduce the material. To view a copy of this license, visit <http://creativecommons.org/licenses/by/4.0/>

© The Author(s) 2016